Received: 20 April 2023 | Revised: 12 September 2023 | Accepted: 11 October 2023

DOI: 10.1111/liv.15767

Liver INTERNATIONAL WILEY

ORIGINAL ARTICLE

FXR agonists INT-787 and OCA increase RECK and inhibit liver steatosis and inflammation in diet-induced ob/ob mouse model of NASH

Laura G. Di Pasqua[1] | Marta Cagna[1] | Giuseppina Palladini[1,2] | Anna C. Croce[3,4] | Massimiliano Cadamuro[5] | Luca Fabris[6,7] | Stefano Perlini[1,8] | Luciano Adorini[9] | Andrea Ferrigno[1] | Mariapia Vairetti[1]

[1]Department of Internal Medicine and Therapeutics, University of Pavia, Pavia, Italy

[2]Internal Medicine Fondazione IRCCS Policlinico San Matteo, Pavia, Italy

[3]Institute of Molecular Genetics, Italian National Research Council (CNR), Pavia, Italy

[4]Department of Biology and Biotechnology, University of Pavia, Pavia, Italy

[5]Department of Medicine (DIMED), University of Padua, Padua, Italy

[6]Department of Molecular Medicine (DMM), University of Padua, Padua, Italy

[7]Department of Internal Medicine, Liver Center and Section of Digestive Diseases, Yale University, New Haven, Connecticut, USA

[8]Emergency Department, Fondazione IRCCS Policlinico San Matteo, Pavia, Italy

[9]Intercept Pharmaceuticals Inc., Morristown, New Jersey, USA

Correspondence
Andrea Ferrigno, Department of Internal Medicine and Therapeutics, University of Pavia, Via Ferrata 9, 27100 Pavia, Italy.
Email: andrea.ferrigno@unipv.it

Funding information
University of Pavia and by Intercept Pharmaceuticals, Inc., Grant/Award Number: FRG20SZ08

Abstract

Background and Aims: We have previously shown in a model of hepatic ischaemia/reperfusion injury that the farnesoid X receptor (FXR) agonist obeticholic acid (OCA) restores reversion-inducing-cysteine-rich protein with Kazal motifs (RECK), an inverse modulator of metalloproteases (MMPs) and inhibitor of the sheddases ADAM10 and ADAM17 involved in inflammation and fibrogenesis. Here, the effects of FXR agonists OCA and INT-787 on hepatic levels of RECK, MMPs, ADAM10 and ADAM17 were compared in a diet-induced ob/ob mouse model of non-alcoholic steatohepatitis (NASH).

Methods: Lep ob/ob NASH mice fed a high-fat diet (HFD) or control diet (CD) for 9 weeks (wks) were treated with OCA or INT-787 0.05% dosed via HFD admixture (30 mg/kg/day) or HFD for further 12 wks. Serum alanine transaminase (ALT) and inflammatory cytokines, liver RECK, MMP-2 and MMP-9 activity as well as ADAM10, ADAM17, collagen deposition (Sirius red), hepatic stellate cell activation (α-SMA) and pCK^+ reactive biliary cells were quantified.

Results: Only INT-787 significantly reduced serum ALT, IL-1β and TGF-β. A downregulation of RECK expression and protein levels observed in HFD groups (at 9 and 21 wks) was counteracted by both OCA and INT-787. HFD induced a significant increase in liver MMP-2 and MMP-9; OCA administration reduced both MMP-2 and MMP-9 while INT-787 markedly reduced MMP-2 expression. OCA and INT-787 reduced both ADAM10 and ADAM17 expression and number of pCK^+ cells. INT-787 was superior to OCA in decreasing collagen deposition and α-SMA levels.

Abbreviations: AF, autofluorescence; ALP, alkaline phosphatase; BAs, bile acid; CD, control diet; CMC, critical micellar concentration; ECM, extracellular matrix; FXR, farnesoid X receptor agonist; HFD, high-fat diet; HPCs, hepatic progenitor cells; HSC, hepatic stellate cell; I/R, ischaemia/reperfusion; IL-1β, interleukin-1β; MMPs, metalloproteases; OCA, obeticholic acid; RECK, reversion-inducing-cysteine-rich protein with Kazal motifs; SHP, small heterodimer partner; TGF-β, transforming growth factor β; TGR5, Takeda G protein-coupled BA protein 5 receptor.

Laura G. Di Pasqua and Marta Cagna are contributed equally to this study.

Handling Editor: Luca Valenti

Conclusion: INT-787 is superior to OCA in controlling specific cell types and clinically relevant anti-inflammatory and antifibrotic molecular mechanisms in NASH.

KEYWORDS
ADAMs, FXR, INT-787, NASH, OCA, RECK

1 | INTRODUCTION

Non-alcoholic steatohepatitis (NASH), an advanced stage of non-alcoholic fatty liver disease (NAFLD), is characterized by hepatic steatosis, hepatocyte damage and inflammation, leading to fibrosis, liver cirrhosis and hepatocellular carcinoma.[1] NASH pathogenesis involves multiple pathways responsible for different parallel hits, including lipotoxicity caused by free fatty acids (FFAs) and their derivatives combined with mitochondrial dysfunction[2] as well microbiota dysbiosis, with bacterial species differentiating NAFLD and NASH patients,[2] in addition to pro-inflammatory and pro-fibrotic pathways.[1,2]

NASH represents a major unmet medical need, but no pharmacological treatments have yet been approved. Among the therapeutic opportunities offered by the different mechanisms involved in NASH development, farnesoid X receptor (FXR) activation has emerged as an established pharmacological target, as documented by various FXR agonists in advanced clinical development.[3]

FXR activation reduces bile acid (BA) production by inhibiting the rate-limiting enzyme in the conversion of cholesterol into BAs, CYP7A1, via the FXR-small heterodimer partner (SHP) axis, and by indirect extra-hepatic signalling of FXR-induced FGF19 (human) and FGF15 (rodent) in the intestine, suppresses hepatocellular BA uptake via downregulation of BA uptake transporters (NTCP) and favours BA export via stimulation of sinusoidal (OSTα/β) and canalicular (MRP2, BSEP) BA transporters.[4] FXR activation promotes intestinal barrier integrity by inducing genes involved in the acute phase of mucosal immune response (Ang1) and reducing bacterial translocation and subsequent inflammation.[5] FXR agonists lower plasma glucose levels via repression of gluconeogenesis, favouring glucose disposition and glycogen storage.[4] In addition, FXR activation inhibits the transcription factor for lipogenic pathways SREBP-1c, and thereby reduces key enzymes for de novo lipogenesis as well as exerting trans-repressive effects on inflammation by inhibiting the transcription factor NF-κB thus reducing pro-inflammatory cytokines such as TNFα, IL-1β and IL-6 and inhibiting the NLRP3 inflammasome. Moreover, FXR activation modulates hepatic stellate cell (HSC) activation, inhibits trans-differentiation and contractility of HSCs and improves vascular inflammation and remodelling.[5]

We have previously shown that the FXR agonist obeticholic acid (OCA) significantly reduces metalloproteases (MMPs) 2 and 9 both in the liver and bile.[6] Hepatic MMPs play a role in NASH fibrogenesis, contributing not only to the balance between formation and degradation of connective tissue components but also to signal transduction for tissue recovery.[7] Furthermore, OCA modulates MMP-2 and TIMP-1 expression in HSCs and promotes the resolution of liver fibrosis.[8] MMPs are negatively regulated by reversion-inducing-cysteine-rich protein with Kazal motifs (RECK), a protease inhibitor-like molecule anchored to the plasma membrane, expressed in a wide variety of normal human tissues.[9] The key action of RECK is to regulate MMPs involved in the breakdown of extracellular matrix (ECM) and angiogenesis.[9]

Members of the disintegrin and metalloprotease (ADAM) family are also involved in ECM remodelling.[10] The various ADAM family members seem to play different roles during hepatic fibrosis modulating pro- and anti-fibrotic processes.[11] In addition to MMPs, RECK is also a known inhibitor of ADAM17 and ADAM 10. ADAM17 is a type 1 transmembrane metalloprotease with wide tissue expression, facilitating cleavage and release of a variety of substrates involved in both the initiation and propagation of inflammation.[11] While definitive experimental proof is still lacking, it is likely that ADAM17 is essential for the establishment of hepatic inflammation and the development of liver fibrosis, as well as being implicated in hepatocyte apoptosis and activation of HSCs,[10] the major source of ECM in liver fibrosis.[11] ADAM10 appears also to be an important regulator of liver homeostasis. A study by Muller et al. reported that in an ADAM10-deficient mouse model, loss of hepatic ADAM10 results in hepatocyte necrosis.[12] In addition, ADAM10, ADAM17 and MMP-2 synthesized by activated HSCs mediate CX3CL1 shedding and release of chemotactic peptides, thereby facilitating the recruitment of inflammatory cells and paracrine stimulation of HSCs in chronic liver diseases.[13] RECK has been shown to inhibit ADAM10 expression, demonstrating to be also involved in the regulation of pro-inflammatory signalling cascade and in HSC activation[14] This may, at least in part, be due to an accumulation of liver progenitor cells that have previously been linked to HSC activation.[11]

Interestingly, we have recently found that OCA treatment is able to increase RECK protein expression in rat livers submitted to hepatic ischemia/reperfusion (I/R) damage.[6] Based on these results,

Lay summary

INT-787 is superior to OCA in reducing inflammation and fibrosis by controlling cellular and molecular drivers involved in pathogenesis and progression from NAFLD to NASH. RECK is an innovative, potentially clinically relevant, target inhibiting inflammatory and fibrogenic processes, via MMPs and ADAMs, in NASH.

the aim of the present study was to assess the ability of OCA and INT-787 to inhibit liver inflammation and fibrosis by upregulating RECK expression with consequently reduced MMP activity and ADAM levels in ob/ob mice treated with a high-fat diet (HFD), an experimental model of NASH.

2 | MATERIALS AND METHODS

2.1 | Animal model

Male B6V-LEP (ob/ob) mice, 6 weeks (wks) old, were obtained from Charles River Laboratories (Italy) and housed under standardized conditions (24 ± 2°C; 12 h light–dark cycle). Mice were administered for 9 wks an HFD, (AMLN diet D09100301, manufactured by Laboratorio-Dottori-Piccioni, Gessate, Italy) or a control diet (CD) (D09100304). (Diet formulations are shown in Table S1). Mice were divided into 5 groups: (1) CD 21 wks (9 + 12 wks) ($n = 7$); (2) HFD 9 wks ($n = 6$); (3) HFD 9 wks followed by HFD + vehicle for 12 wks ($n = 10$); (4) HFD 9 wks followed by HFD + OCA 30 mg/kg for 12 wks ($n = 10$); (5) HFD 9 wks followed by HFD + INT-787 30 mg/kg for 12 wks ($n = 10$). All procedures involving animals were approved by the Italian Ministry of Health and by the University Commission for Animal Care (Protocol number 753/2020-PR). Baseline (9 wks) and terminal (21 wks) samples (liver left lobes and serum) collected in anaesthetised mice (sodium pentobarbital 40 mg/kg i.p.) were snap-frozen in liquid nitrogen for further evaluation. Liver samples have been fixed in paraformaldehyde for histology analysis.

2.2 | Real-time qPCR

RECK, MMPs, TIMPs and TGF-β mRNA expression were analysed by RT-qPCR. Total RNA was isolated from the liver homogenized in TRI reagent (Sigma-Aldrich, Milan, Italy), in accordance with the method described by Chomczynski et al.[15] Further details can be found in the Supplementary Materials.

2.3 | ELISA detection kits

Serum interleukin-1β (IL-1β), transforming growth factor-β (TGF-β) and ADAM-10 were measured using ELISA kits (Invitrogen, Abcam and MyBiosource, respectively), according to the instructions, and analysed with a microplate reader (Bio-Rad, model 550).

2.4 | Gelatin zymography

Protein extraction from snap-frozen samples and gelatin zymography were performed as previously described.[6] To detect MMP lytic activity, solubilized proteins were loaded onto electrophoretic gels (SDS-PAGE), containing 1 mg/mL gelatin, under non-reducing conditions. After run and incubation for 18 h at 37°C dedicated buffer gels were stained with Coomassie Brilliant Blue to reveal zones of lysis. Zymograms were analysed by a densitometer (GS 900 Densitometer Bio-Rad).

2.5 | Western immunoblots

Liver tissue samples were homogenized in lysis buffer with a protease inhibitor cocktail. The cleaved proteins (RECK, eNOS, ADAM10, ADAM17 and α-SMA) were separated in SDS-PAGE on 7.5% acrylamide gels and transferred to PVDF membrane (Bio-Rad). After blocking in 5% BSA for 2 h, the membranes were incubated with primary antibodies (RECK and ADAM10: Santa Cruz Biotechnology; eNOS: Cayman Chemical; ADAM17 and GAPDH: Invitrogen; a-SMA: cell signalling Technologies; Tubulin: Merck Millipore) overnight at 4°C and then incubated with peroxidase-conjugated secondary anti-rabbit or anti-mouse antibodies Santa Cruz Biotechnology. Immunostaining was revealed with BIO-RAD Chemidoc XRS+, visualized using the ECL Clarity (BIO-RAD), and intensity quantification performed by Image Lab Software™6.0.1 (Bio-Rad).

2.6 | Immunofluorescence staining

Acetone-fixed, 4 μm thick, cut frozen liver sections, were treated for 8 mins with UltraVision ProteinBlock (ThermoFisher Scientific), and then immunostained by overnight incubation at 4°C with rabbit polyclonal anti-wide spectrum screening cytokeratins (pCK, Agilent) and anti-RECK (Santa Cruz Biotechnology). Following incubation, slides were rinsed, incubated with the appropriate secondary antibody (Alexa fluor 488 or 594, ThermoFisher Scientific) and then mounted with ProLong Gold with DAPI (ThermoFisher Scientific) antifade mounting media. Primary and secondary antibodies have been diluted using phosphate buffer saline 1× (PBS, Euroclone) supplemented with 0.5% bovine serum albumin (BSA). Immunofluorescence was detected with an Eclipse E800 microscope, equipped with a DS-U1 cooled digital camera, and analysed with LuciaG software (Nikon). Morphometric analysis was used to quantify biliary structures and hepatic progenitor cells (HPCs) according to the categorization of Roskams et al.[16] Reactive biliary cells were defined as pCK^+ structures arranged in irregularly shaped structures inside the portal area or at the portal interface. Extent of pCK^+ structures was calculated as percentage of pixels above the threshold value with respect to the total pixels of the area, while HPCs were counted. Both analyses were performed in 5 non-overlapping, randomly selected fields/sample (objective 100×).

2.7 | Lipid accumulation

The hepatic lipid accumulation was evaluated by histological analysis: semiquantitative morphometric analysis of number, area and

diameter of lipid droplets was evaluated on haematoxylin and eosin-stained sections, using Image-J software.

2.8 | Liver fibrosis

Fibrous collagen was evidenced by Sirius red (Direct Red 80, Sigma-Aldrich) staining. Liver samples embedded in Paraplast and sliced into 8-μm-thick sections were stained with picrosirius red solution and mounted for microscope observation under bright field conditions (Nikon Eclipse E800) by using the UPlanFL-10X and UPlanFL-20X objectives.

2.9 | Autofluorescence analysis

Progression of liver fibrosis was assessed by estimating collagen autofluorescence (AF) by ex vivo spectrofluorometric and imaging analysis performed on liver tissue cryostatic sections to investigate the network organization of the fluorescing reticular fibres and collagen proteins.[17,18] Further details can be found in the Supplementary Materials.

2.10 | Serum biochemistry

Serum alanine transaminase (ALT), alkaline phosphatase (ALP), total bilirubin, cholesterol, triglycerides and BAs were quantified by an automated Beckman Coulter AU 5820 according to the manufacturer's instructions.

2.11 | Statistical analysis

Data are presented as means ± SEM. Differences among the 5 groups were estimated by one-way ANOVA followed by Tukey's test for multiple comparisons. When data distribution was not normal Kruskal–Wallis and Dunn's test were used. Association between parameters was evaluated according to Pearson correlation (normally distributed variables) or Spearman rank correlation (not normally distributed variables). In the graphs, letters a–c indicate $p < 0.05$ comparing OCA versus Control 21 wks, HF 9 wks and HF 21 wks, respectively; letters d–f indicate $p < 0.05$ comparing INT-787 versus Control 21 wks, HF 9 wks and HF 21 wks, respectively; letter g indicates $p < 0.05$ OCA versus INT-787. Letters h–j indicate $p < 0.01$ comparing OCA versus Control 21 wks, HF 9 wks and HF 21 wks, respectively; letters k, l, and m indicate $p < 0.01$ comparing INT-787 versus Control 21 wks, HF 9 wks and HF 21 wks respectively; letter n indicates $p < 0.01$ OCA versus INT-787. Letters o, p and q indicate $p < 0.001$ comparing OCA versus Control 21 wks, HF 9 wks and HF 21 wks, respectively; letters r, s and t indicate $p < 0.001$ comparing INT-787 versus Control 21 wks, HF 9 wks and HF 21 wks, respectively; letter u indicates $p < 0.001$ OCA versus INT-787. Statistical analysis was performed using MedCalc Statistical Software (version 18.11.3).

3 | RESULTS

3.1 | Effects of OCA and INT-787 treatment on liver injury and lipid regulation

INT-787, a novel OCA derivative hydroxylated at position C11β, is equipotent to OCA at FXR but with no agonistic activity for the Takeda G protein-coupled BA protein 5 receptors (TGR5), as reported in Table S3 based on data from Pellicciari et al.[19] INT-787 shows high FXR selectivity at concentrations up to 100 μM with no co-regulator recruitment activities, as well as a 16-fold higher water solubility than OCA and a high critical micellar concentration (CMC) resulting in mild detergency and reduced toxicity.[19] About 50% of the administered INT-787 dose is recovered unmodified in bile, indicating efficient biliary uptake and biliary secretion. Its relatively low lipophilicity is responsible for this efficient secretion compared with OCA, which requires full conjugation with taurine or glycine to be secreted into bile.[19] Efficiency of INT-787 versus OCA for selected FXR target genes was determined by Pellicciari et al.[19] in HepG2 cells. Both compounds were equipotent in modulating Cyp7a1, Shp, and Ostα while Bsep was upregulated more efficiently by INT-787 (Table S4). In vivo studies in C57BL/6 mice showed that INT-787-dependent activation of FXR intestinal targets Fgf15 and Ang1 was markedly higher than OCA (Table S4), whereas hepatic Cyp7a1 expression was inhibited equally well by OCA and INT-787 treatment (Table S4).[19]

A diet-induced ob/ob mouse model of NASH was used to evaluate the therapeutic effects of OCA and INT-787. The compound dose of 30 mg/kg/day was determined according to Roth et al.[20] OCA and INT-787 treatment reduced liver weight compared with HFD-treated mice at 9 and 21 wks, and liver weight in INT-787-treated mice was comparable to the CD group (Figure 1B). The livers of mice treated with FXR agonists appeared reddish-brown while those from HFD 9 and 21 wk groups were pale in colour.[21] INT-787 administration reduced serum levels of ALT compared with all other groups (Figure 1C). An increase in serum ALP was found with HFD after 9 wks but no differences with the CD group were observed in HFD 21 wks and after OCA or INT-787 treatment (Figure 1C). OCA and INT-787 treatment reduced serum bilirubin and BAs compared with HFD 9 and 21 wks (Figure 1C). Serum cholesterol increased in HFD 9 and 21 wks mice compared with the CD group but OCA and INT-787 administration markedly counteracted these increases (Figure 1C). No changes in serum triglycerides were found in any group considered (Figure S1).

Histological analysis showed accumulation of a large number of lipid droplets in the liver of HFD 9 and 21 wks compared with the CD group, and INT-787 treatment normalized the number of lipid droplets, compared with HFD at 9 and 21 wks and OCA group, to values similar to those found in CD mice (Figure 2A,B). Quantification of lipid droplet area and diameter showed an accumulation of large lipid droplets in HFD mice after 9 and 21 wks

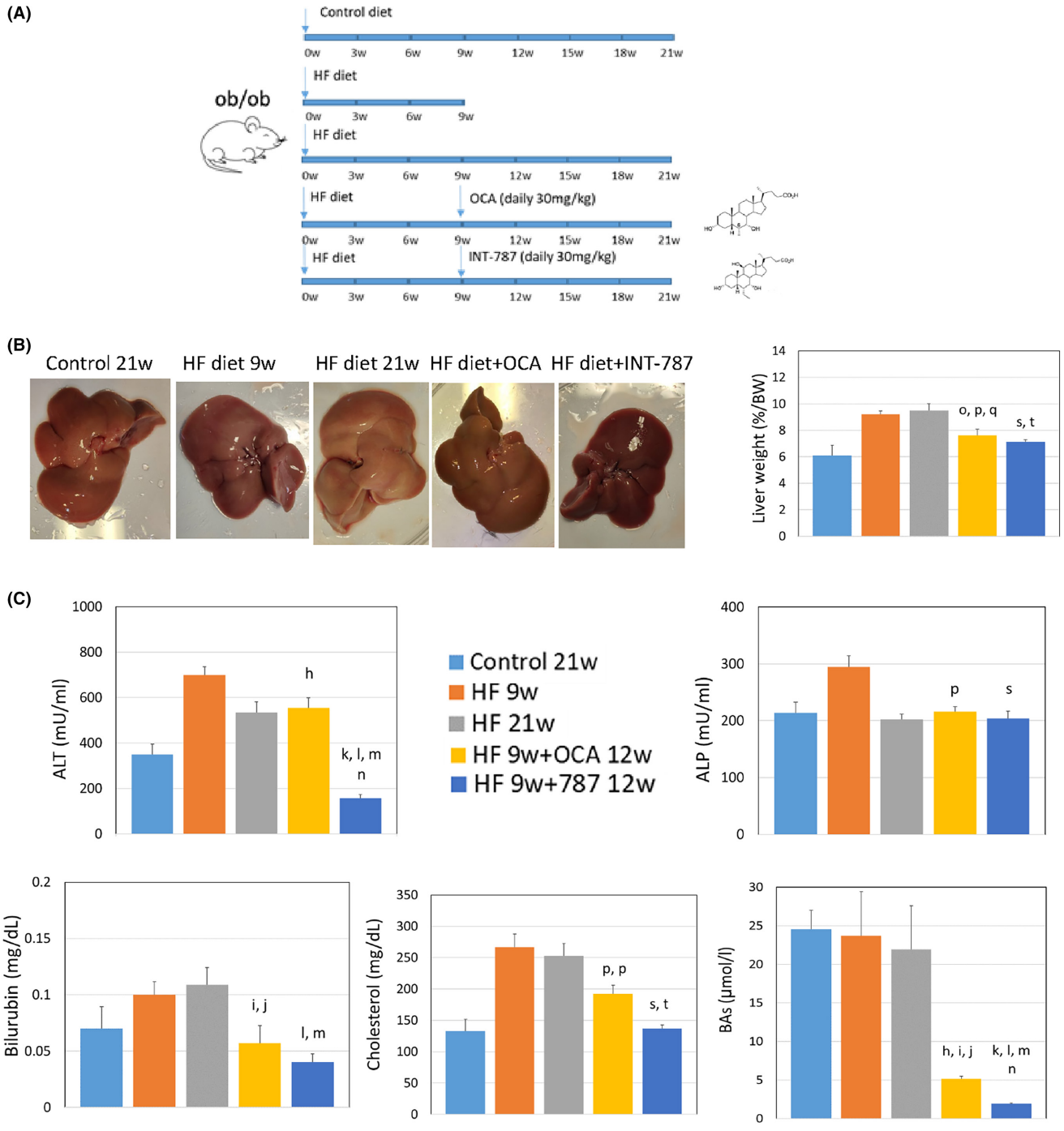

FIGURE 1 Effect of obeticholic acid (OCA) and INT-787 on liver injury in a diet-induced ob/ob mouse model of non-alcoholic steatohepatitis (NASH). (A) Experimental groups and treatments; (B) representative liver aspect in mice of experimental groups and liver/body weight ratio; (C) serum levels of alanine transaminase (ALT), alkaline phosphatase (AP), bilirubin, cholesterol and bile acids (BAs). Data are shown as mean ± SEM. Letters h–j indicate $p < 0.01$ comparing OCA versus control 21 weeks (w), HF 9 w and HF 21 w, respectively; letters k–m indicate $p < 0.01$ comparing INT-787 versus Control 21 w, HF 9 w and HF 21 w, respectively; letter n indicates $p < 0.01$ OCA versus INT-787. Letters p, q indicate $p < 0.001$ comparing OCA versus HF 9 w and HF 21 w, respectively; letters s and t indicate *rsu* < 0.001 comparing INT-787 versus HF 9 w and HF 21 w, respectively.

compared with the CD group; OCA and INT-787 normalized area and diameter of lipid droplets to values comparable to those found in CD group (Figure 2A,B). These data clearly show that INT-787 is superior to OCA in decreasing number, area and diameter of hepatic lipid droplets.

3.2 | OCA and INT-787 increase hepatic RECK expression and reduce metalloproteases

A downregulation of liver RECK protein was observed in the HFD 9-week group and although not significantly also in the 21-wk group

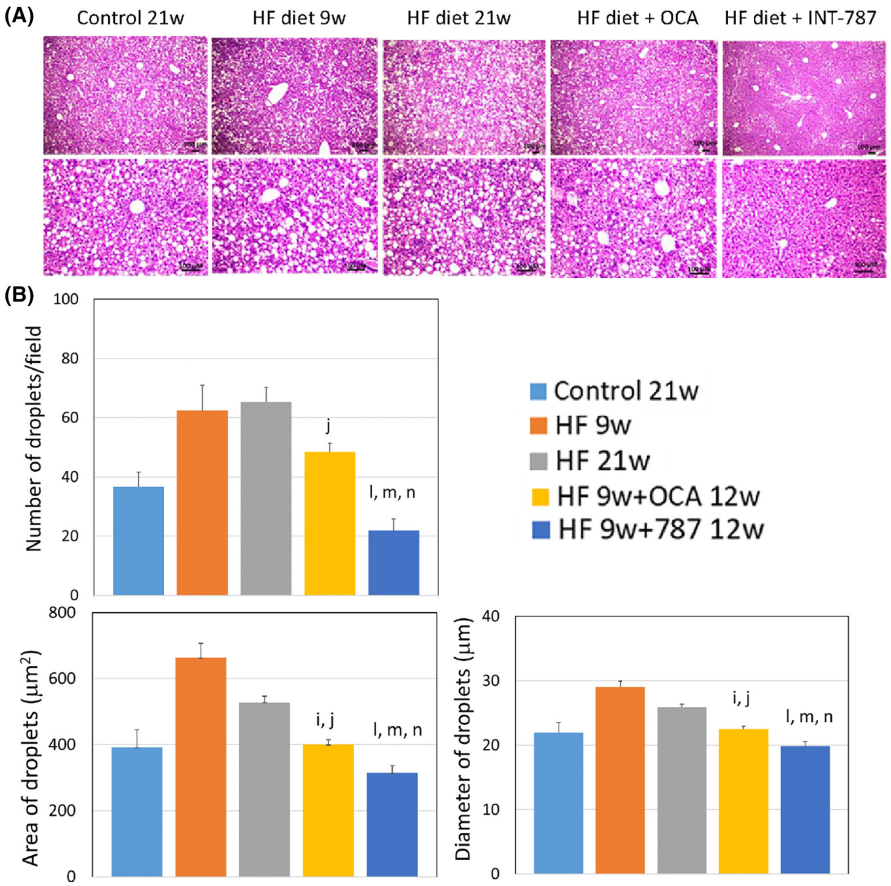

FIGURE 2 Effect of obeticholic acid (OCA) and INT-787 on lipid accumulation in a diet-induced ob/ob mouse model of non-alcoholic steatohepatitis. (A) Representative microscopic images of HE-stained liver sections (scale bar = 0.1 mm); (B) quantification of number, area and diameter of lipid droplets. Data are shown as mean ± SEM. Letters i, j indicate $p < 0.01$ comparing OCA versus HF 9 weeks (w) and HF 21 w, respectively; letters l, m indicate $p < 0.01$ comparing INT-787 versus HF 9 w and HF 21 w, respectively; letter n indicates $p < 0.01$ OCA versus INT-787.

versus CD group (Figure 3A). OCA and INT-787 markedly increased RECK mRNA expression compared to HFD 9 and 21-wk groups and to CD mice (Figure 3A), and INT-787 was significantly superior to OCA in increasing RECK mRNA expression. Consistent with transcript analysis, OCA and INT-787 upregulated RECK protein to values higher than the CD group (Figure 3A). RECK downregulation was also confirmed by double immunofluorescence in liver samples from HF-treated mice compared to controls and to OCA and INT-787-treated mice (Figure 3B), with OCA and INT-787-treated mice showing an intense peribiliary expression of RECK (Figure 3B).

Although not significantly, HFD for 21 wks increased liver MMP-9 activity compared to CD mice, whereas OCA administration normalized it to levels observed in CD mice. Conversely, INT-787 treatment significantly increased MMP-9 activity compared to OCA. In contrast, no significant changes were observed for MMP-9 mRNA expression (Figure 3C). INT-787 administration reduced MMP-2 mRNA expression compared to all other groups (Figure 3C). Significantly increased MMP-2 activity occurred in HFD 21 wks compared with HFD 9 wks and CD group (Figure 3C), whereas MMP-2 activity was decreased by OCA and INT-787 administration (Figure 3C).

3.3 | OCA and INT-787 reduce liver fibrosis

Evaluation of collagen deposition demonstrated its accumulation in livers of HFD mice after 9 and 21 wks compared with the CD group; OCA and INT-787 reduced collagen deposition to values similar to those found in the CD group, and INT-787 was significantly superior to OCA (Figure 4A,C). The relationship of cholesterol and BA levels with fibrosis reduction (Sirius red area) showed a significant positive correlation (Rho 0.588, $p < 0.05$ and Rho 0.641, $p < 0.05$, respectively).

The autofluorescence (AF) of biological substrates can provide label-free information on specific endogenous fluorophores. Images recorded in observation conditions favouring the green emission were recently demonstrated to reveal the morphology of the liver reticular structure.[18] In the present study, AF analysis showed that INT-787 and OCA decrease the hepatic network of fluorescing reticular fibres (Figure 4B). Spectra recorded under 366 nm excitation allowed to estimate the AF of collagenous proteins, demonstrating an increase after 9 and 21 wks of HFD compared with the CD group and a significant decrease, returning to CD values, after INT-787 or OCA administration compared with HFD 9 and 21 wks (Figure 4C).

INT-787 administration markedly reduced TIMP-1 mRNA expression, an index of liver fibrosis,[22] compared to all other groups (Figure 4D). TIMP-2 mRNA levels increased in HFD 21 wks compared with the HFD 9 wks and CD group, and were reduced by INT-787 administration (Figure 4D). Liver TGF-β mRNA expression, a marker of liver fibrosis, was also reduced after INT-787 administration compared with 9 wks of HFD (Figure 4D).

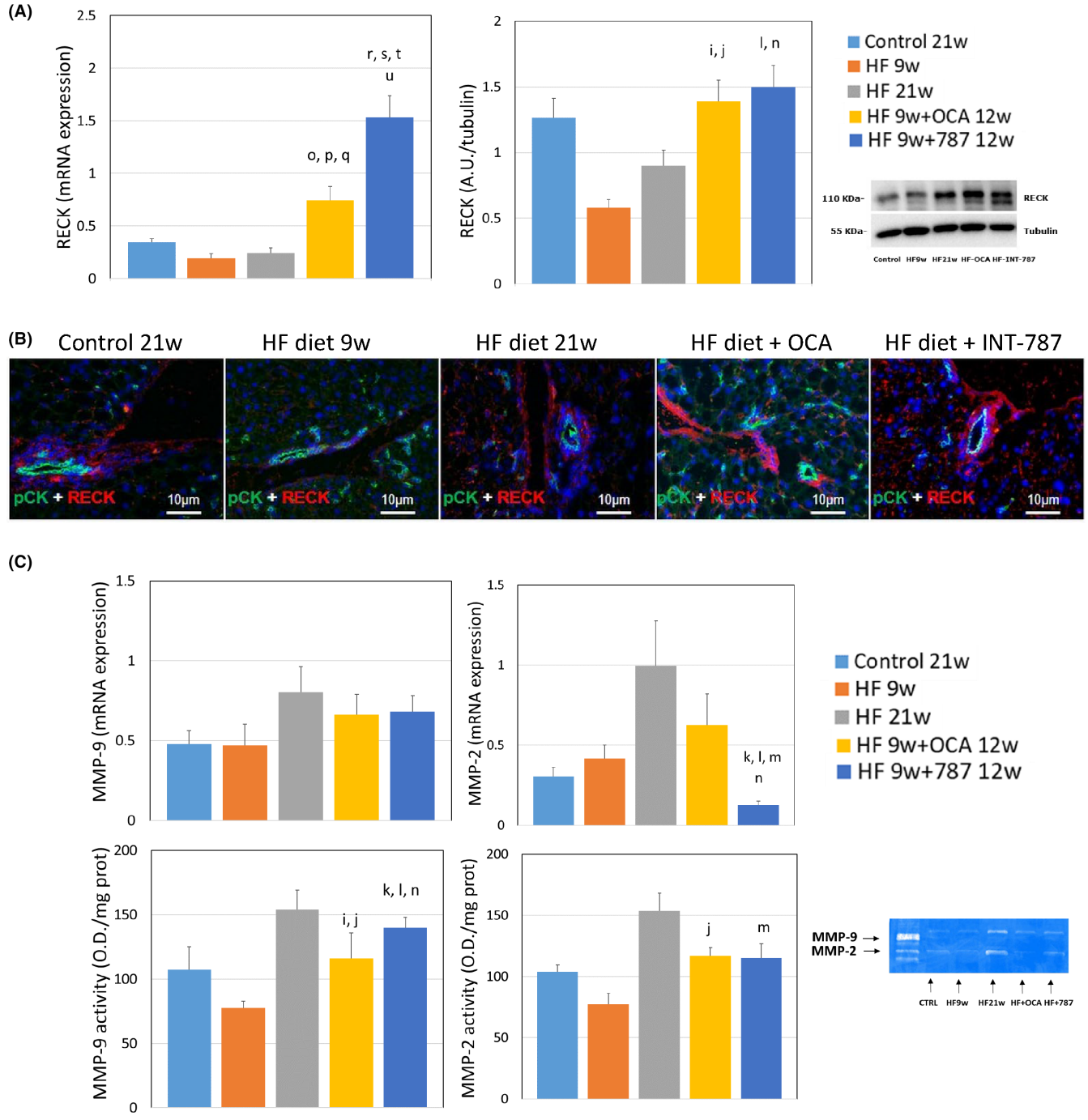

FIGURE 3 In vivo treatments with obeticholic acid (OCA) and INT-787 increase hepatic RECK expression and reduce modulator of metalloproteases (MMPs) in a diet-induced ob/ob mouse model of non-alcoholic steatohepatitis. (A) Hepatic rich protein with Kazal motifs (RECK) mRNA and protein levels; (B) representative microscopic images of RECK-stained liver sections (scale bar = 0.1 mm); (C) quantification of MMP-9 and MMP-2 mRNA and protein levels. Data are shown as mean ± SEM. Letters i, j indicate $p < 0.01$ comparing OCA versus HF 9 weeks (w) and HF 21 w, respectively; letters k–m indicate $p < 0.01$ comparing INT-787 versus control 21 w, HF 9 w and HF 21 w, respectively; letter n indicates $p < 0.01$ OCA versus INT-787. Letters o–q indicate $p < 0.001$ comparing OCA versus control 21 w, HF 9 w and HF 21 w, respectively; letters r–t indicate $p < 0.001$ comparing INT-787 versus control 21 w, HF 9 w and HF 21 w, respectively; letter u indicates $p < 0.001$ OCA versus INT-787.

3.4 | INT-787 reduces serum IL-1β and TGF-β and enhances hepatic eNOS and ATP levels

IL-1 family cytokines are the main drivers of inflammation.[23] A reduction in serum IL-1β was induced by INT-787 treatment versus HFD 9 wks mice and OCA-treated group (Figure 5A). INT-787 administration also reduced serum TGF-β levels, which were increased in mice treated with HFD for 9 and 21 wks (Figure 5A).

The emerging role of eNOS in the regulation of liver vascular tone has been described to be associated with NASH development.[24]

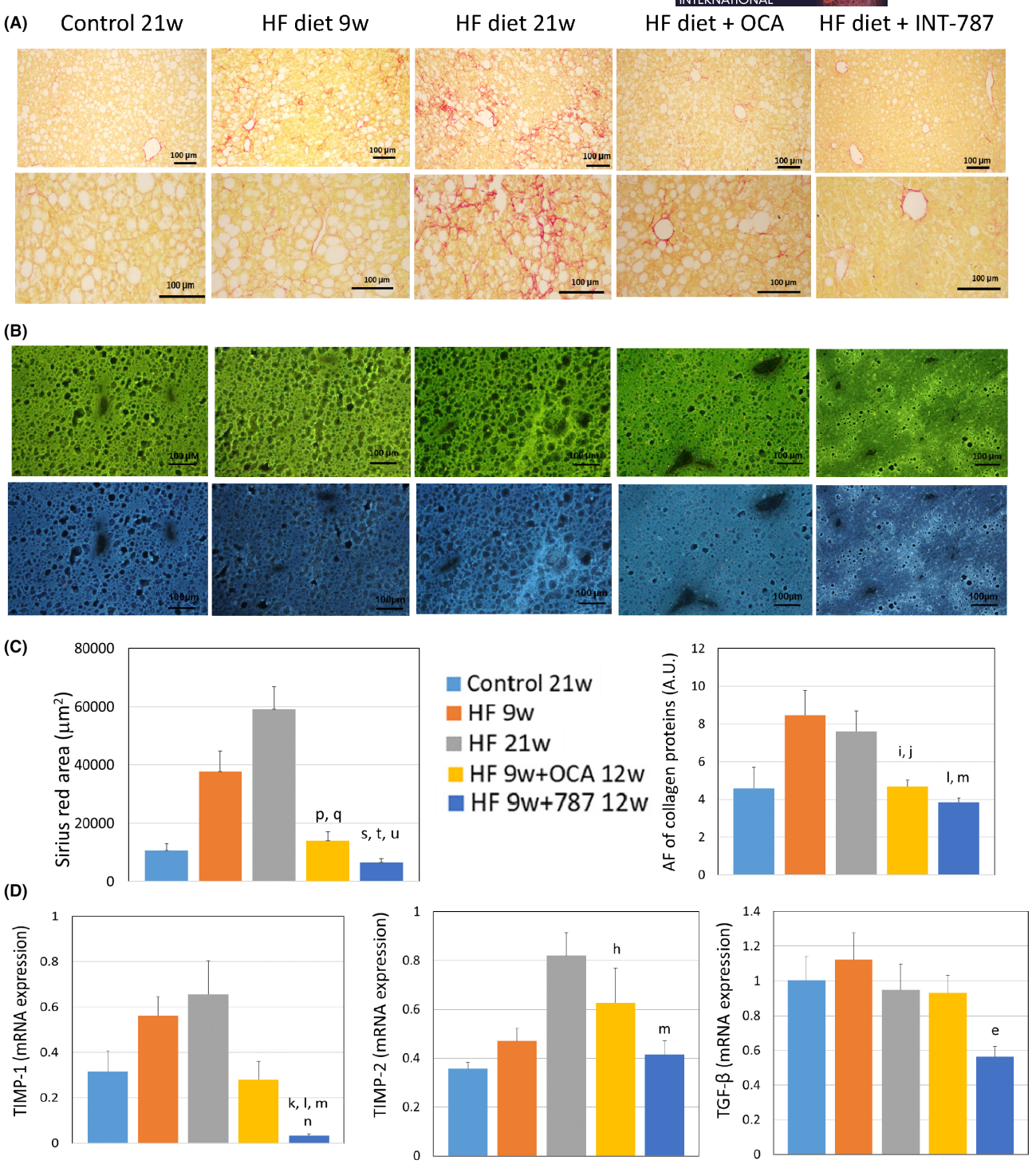

FIGURE 4 Obeticholic acid (OCA) and INT-787 reduce liver fibrosis in a diet-induced ob/ob mouse model of non-alcoholic steatohepatitis. (A) Representative microscopic images of Sirius red-stained liver sections (scale bar = 0.1 mm); (B) representative microscopic images of green and blue autofluorescence (AF) liver sections (scale bar = 0.1 mm); (C) quantification of Sirius red positive area and green and blue autofluorescence of liver section; (D) hepatic mRNA expression of TIMP-1, TIMP-2 and TGF-β. Data are shown as mean ± SEM. Letter e indicates $p < 0.05$ comparing INT-787 versus HF 9 weeks (w). Letters h–j indicate $p < 0.01$ comparing OCA versus control 21 w, HF 9 w and HF 21 w, respectively; letters k–m indicate $p < 0.01$ comparing INT-787 versus control 21 w, HF 9 w and HF 21 w, respectively; letter n indicates $p < 0.01$ OCA versus INT-787. Letters p, q indicate $p < 0.001$ comparing OCA versus HF 9 w and HF 21 w, respectively; letters s, t indicate $p < 0.001$ comparing INT-787 versus HF 9 w and HF 21 w, respectively; letter u indicates $p < 0.001$ OCA versus INT-787.

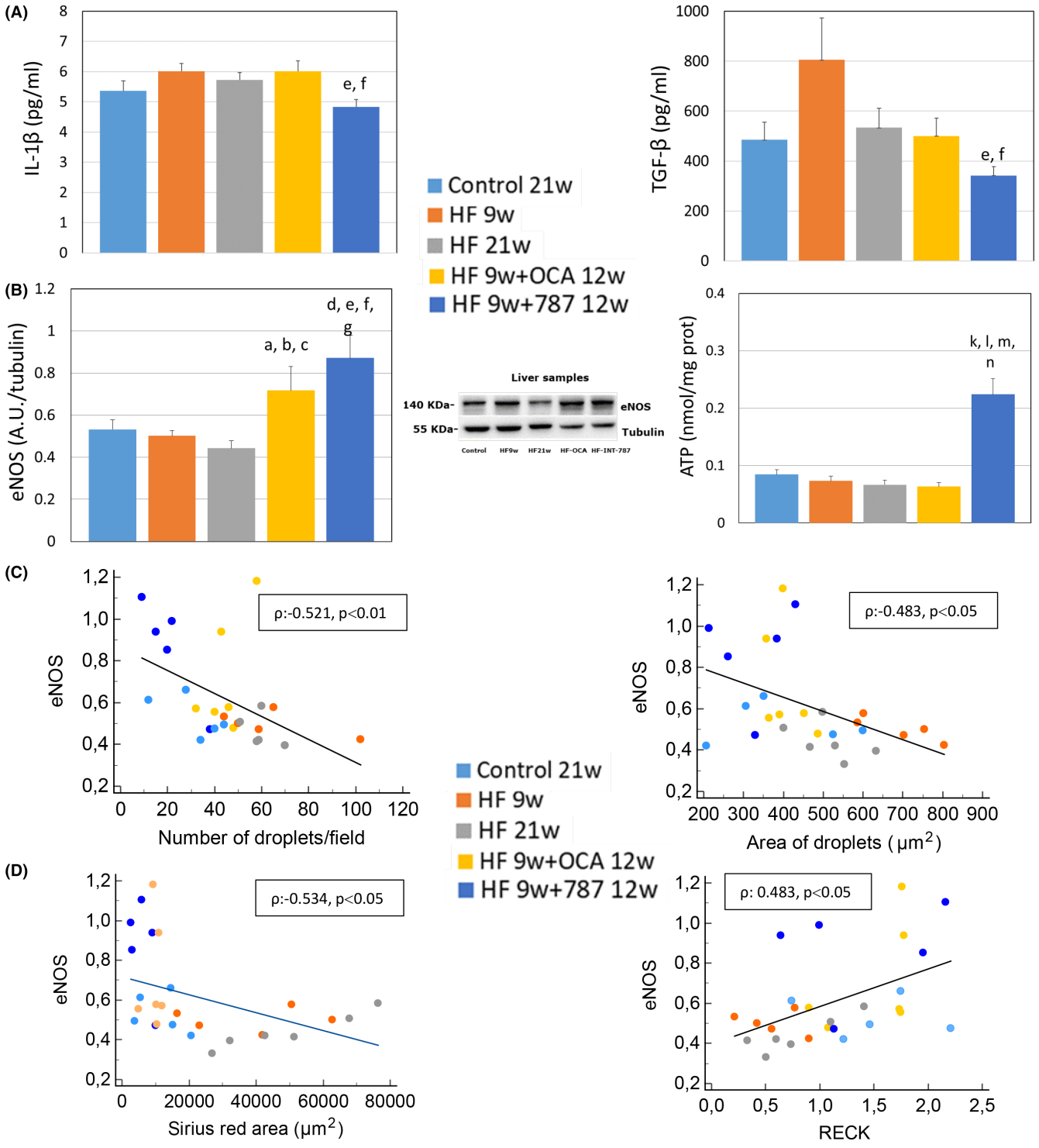

FIGURE 5 INT-787 reduces serum IL-1β and TGF-β and enhances hepatic eNOS and ATP levels in an HFD-induced ob/ob mouse model of non-alcoholic steatohepatitis. (A) Serum IL-1β and TGF-β levels, (B) hepatic eNOS and ATP levels, (C) correlation between eNOS versus number and area of lipid droplets, (D) correlation between eNOS versus. Sirius red area and rich protein with Kazal motifs (RECK). Data are shown as mean ± SEM. Letters a–c indicate $p < 0.05$ comparing obeticholic acid (OCA) versus Control 21 w, HF 9 w and HF 21 w, respectively; letters d–f indicate $p < 0.05$ comparing INT-787 versus Control 21 w, HF 9 w and HF 21 w, respectively; letter g indicates $p < 0.05$ OCA versus INT-787. Letters k–m indicate $p < 0.01$ comparing INT-787 versus Control 21 w, HF 9 w and HF 21 w, respectively; letter n indicates $p < 0.01$ OCA versus INT-787.

Here we document that hepatic eNOS increased in the INT-787 group compared with HFD for 9 and 21 wks and also in the OCA group compared with HFD 21 wks (Figure 5B). Higher levels of hepatic ATP were documented only in INT-787 group compared with all the other groups evaluated (Figure 5B). A significant inverse correlation was found comparing liver eNOS versus number and area

of lipid droplets (Figure 5C) and versus Sirius red area (Figure 5D). Conversely, a positive correlation was found when comparing eNOS versus RECK (Figure 5D).

3.5 | OCA and INT-787 reduce the extent of biliary structures but not of HPCs

NASH, as other chronic liver diseases, is characterized by the activation of the hepatic reparative/regenerative machinery composed of reactive ductular cells and HPCs[25] putatively supervising activation of myofibroblasts and fibrosis deposition. To evaluate if treatments with OCA and INT-787 were able to modulate this machinery, the extent of ductular reaction (pCK$^+$ cells) and the number of HPCs were evaluated. Interestingly, while no changes were observed in the activation of HPC compartment (Figure 6B), stimulation with both OCA and INT-787 were able to significantly reduce the extent of pCK$^+$ structures (Figure 6A). These data are in line with Sirius Red staining, as also documented by a significant positive correlation of pCK$^+$ cells with Sirius red area, thus demonstrating the role of OCA and INT-787 in reducing fibrosis deposition (Figure 6A).

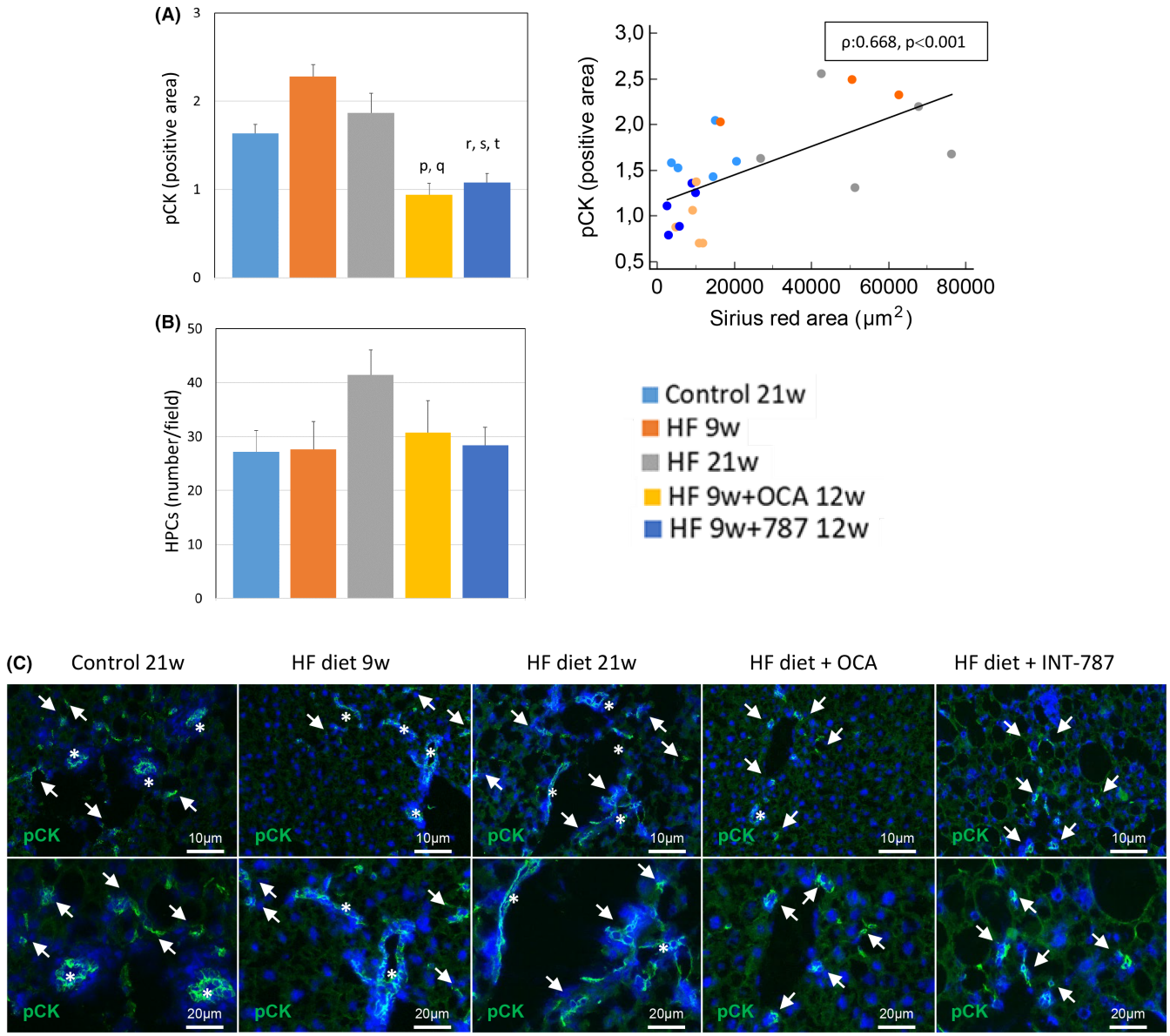

FIGURE 6 In vivo treatments with obeticholic acid (OCA) and INT-787 reduce the extent of biliary structures but not of hepatic progenitor cells (HPC) in the HFD-fed ob/ob mouse model of non-alcoholic steatohepatitis. (A) Quantification of pCK$^+$ biliary structures (green) and correlation between pCK versus sirius red; (B) HPCs number in liver sections from the different treatment cohorts. (C) Representative pictures of liver specimens at the indicated magnifications. Biliary structures are stained in green. White *: reactive ductular cells; white arrows: HPCs. Data are shown as mean ± SEM. Letters p, q indicate $p < 0.001$ comparing OCA versus HF 9 w and HF 21 w, respectively; letters r–t indicate $p < 0.001$ comparing INT-787 versus control 21 w, HF 9 w and HF 21 w, respectively.

3.6 | Inhibition by OCA and INT-787 of ADAM-10 and ADAM-17 levels

Both OCA and INT-787 reduced hepatic ADAM-10 levels, which were slightly upregulated after 9 and 21 wks of HFD (Figure 7A). ADAM-17 levels increased in the HFD group after 21 wks and were significantly decreased by OCA and INT-787 (Figure 7B). In addition, INT-787 reduced hepatic α-SMA which was increased in the 21-wk HFD group (Figure 7B).

4 | DISCUSSION

FXR is the primary sensor of BAs and its role in BA metabolism has been clearly shown by studies in Fxr-null mice demonstrating that FXR is central to control of BA homeostasis and enterohepatic circulation.[26] FXR activation has been shown to reduce NASH features such as steatosis, fibrosis, and hepatocellular death, both in animal models and in NASH patients, by regulating several pathways, including cholesterol and BA homeostasis, hepatic gluconeogenesis, lipogenesis, inflammation and fibrosis.[27]

During hepatic fibrogenesis in NASH, hepatic MMPs play an important role in the balance between formation and degradation of connective tissue components.[28] MMPs are regulated by RECK, a membrane-anchored glycoprotein. RECK, a key regulator of ECM integrity and angiogenesis, inhibits the activity of human MMP-2, MMP-9 and MMP-14 at different steps of their activation cascades.[29,30] Recently, its role in regulating inflammatory and fibrogenic processes has started to emerge. RECK has been identified as a novel transcriptional target gene of FXR and the hepatic RECK downregulation observed in MCD diet mice has been counteracted by FXR activation.[31] Since RECK negatively regulates transcription and secretion of MMP-9 and directly inhibits its enzymatic activity,[29,32] FXR agonists may suppress the activity of MMP-9 by promoting RECK expression. MMP-9 is the critical gelatinase produced by Kupffer cells and is implicated in pathological processes in acute and chronic hepatic injury.[33] Recently, we have observed that OCA administration reduces significantly MMP-2 and MMP-9 activity in the liver and bile.[6] Moreover, we have previously found that OCA is able to increase RECK levels after induction of hepatic I/R injury.[6] Based on these findings, the role of OCA and INT-787 in the resolution of liver fibrosis in NASH has been evaluated. As shown here, FXR activation by INT-787 or OCA administration decreases liver fibrosis and reduces MMP levels associated with RECK upregulation. MMP-2 is highly expressed in myofibroblasts and is considered to play a profibrogenic role.[34]

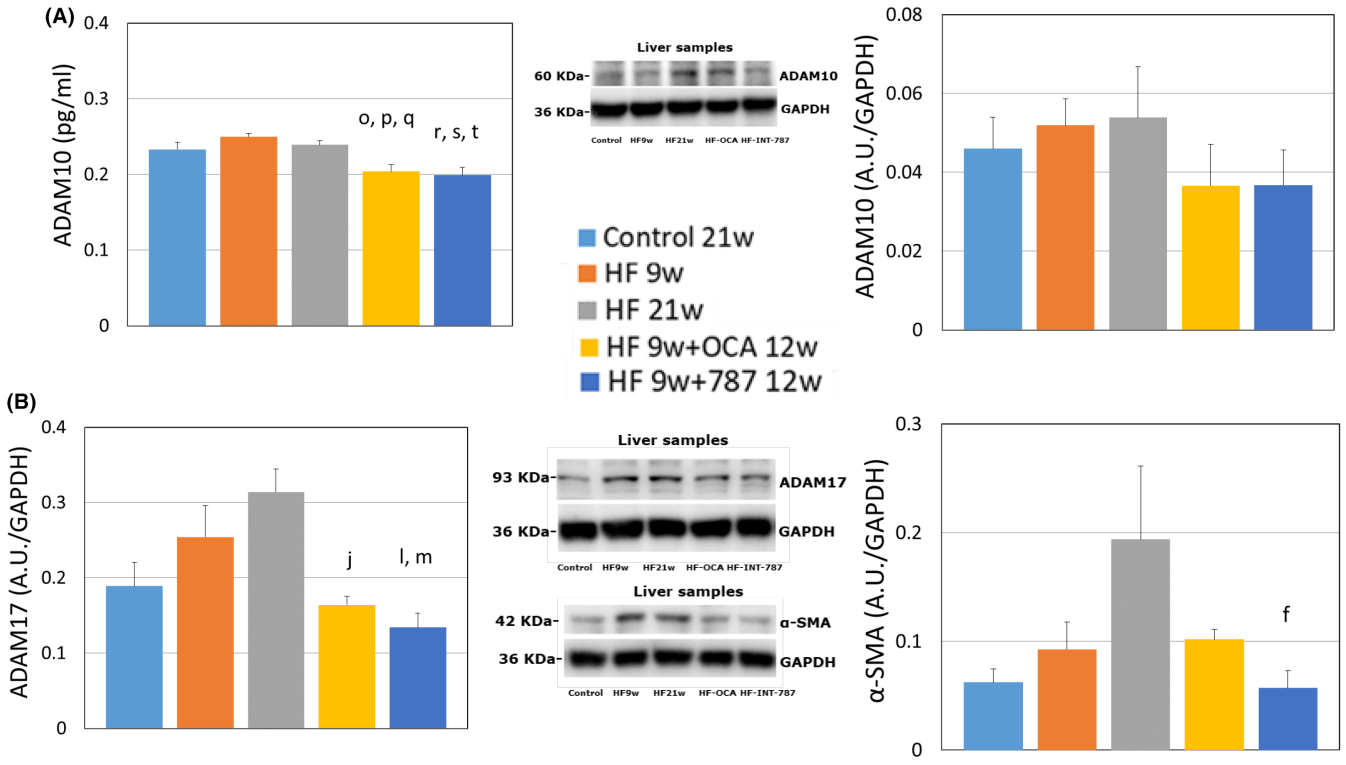

FIGURE 7 Obeticholic acid (OCA) and INT-787 inhibit ADAM-10 and ADAM-17 in HFD-fed ob/ob mouse model of non-alcoholic steatohepatitis. (A) Hepatic ADAM-10 levels evaluated by ELISA (left panel) or Western blot (right panel); (B) Western blot analysis of hepatic ADAM-17 (left panel) and α-SMA (right panel). Data are shown as mean ± SEM. Letter f indicates $p < 0.05$ comparing INT-787 versus HF 21 weeks (w). Letter j indicates $p < 0.01$ comparing OCA versus HF 21 w; letters l and m indicate $p < 0.01$ comparing INT-787 versus HF 9 w and HF 21 w, respectively. Letters o–q indicate $p < 0.001$ comparing OCA versus Control 21 w, HF 9 w and HF 21 w, respectively; letters r–t indicate $p < 0.001$ comparing INT-787 versus Control 21 w, HF 9 w and HF 21 w, respectively.

In our diet-induced ob/ob mouse model of NASH, both OCA and INT-787 counteract the increase in MMP-2 activity and the same trend is also observed for MMP-2 mRNA expression. OCA but not INT-787 administration reduces MMP-9 activity. This is the first study showing reduction of hepatic MMPs associated with upregulation of RECK levels by FXR agonists like OCA and INT-787. The present results are in line with those obtained with OCA in the hepatic I/R injury model.[6] The reduction in MMP activation induced by the administration of FXR agonists is associated with decreased lipid accumulation, fibrosis and HSC activation; key players in hepatic fibrogenesis. INT-787 appears significantly superior to OCA in the reduction of collagen deposition, HSC activation and hepatic steatosis. Only INT-787 reduced serum levels of IL-1β in an MMP-independent manner, demonstrating its efficacy in the inhibition of liver inflammation. Furthermore, serum TGF-β levels and gene expression of TIMP-1 and TGF-β, markers of liver fibrosis, were decreased by INT-787 administration to values comparable with those found in the CD group, indicating its marked capacity to control liver fibrogenesis.

Of note, the increase in RECK induced by INT-787 and OCA is associated with inhibition of the sheddases ADAM10 and ADAM17. This was correlated in the INT-787-treated group to a reduction in the release of proinflammatory cytokines by hepatic cells, which in turn reduced HSC activation. ADAM17 plays a pivotal role in inflammation[35] but identifying a pharmaceutical inhibitor of this enzyme has remained a challenge. In addition to ADAM17, RECK also inhibits ADAM10, and both ADAMs play a critical role in the activation of the pro-inflammatory signalling cascade.[11] As documented in the present study, the ability of FXR agonists OCA and INT-787 to induce RECK has the therapeutic potential to inhibit both ADAM10 and ADAM17, as well as the overt liver inflammation resulting from metabolic dysregulation. Therefore, ADAM proteases might be harnessed therapeutically in the future.

In the present study, the upregulation of RECK was also associated with an increase in eNOS, as documented by a significant positive correlation between these two variables. Recent data have demonstrated the emerging role of eNOS in the regulation of liver vascular tone, strongly associated with NAFLD progression to NASH.[24] A clinical study revealed an important role for hepatocyte-specific eNOS as a key regulator of NAFLD/NASH susceptibility and mitochondrial quality control with direct correlation to NASH.[36] The high levels of hepatic ATP we observed in INT-787-treated mice support the hypothesis suggesting eNOS as a key regulator of NAFLD/NASH susceptibility.

The benefits expected by using INT-787 over OCA in NASH patients are increased protection against NASH-associated liver injury, documented in our study by lower serum ALT levels, higher tissue eNOS and ATP content, as well as superiority in the control of hepatic lipid accumulation, inflammation and fibrogenesis. The advantage of using INT-787 over OCA is also demonstrated by the ability of INT-787 but not OCA to reduce the inflammation index and increase the preservation of mitochondrial functionality to generate ATP.

FXR agonists control the intestinal barrier integrity, preventing bacterial translocation and maintaining the gut microbiota eubiosis.[37] As observed in different chronic metabolic diseases, NASH is associated with gut dysbiosis.[38] Recently, the gut microbiota has been shown to regulate BA metabolism with various mechanisms, thus influencing NASH development.[39] In turn, gut microbiota composition is affected by BA levels.[40] OCA treatment, in an HFD mouse model, increased the abundance of several bacteria groups but also significantly reduced the proportion of four specific bacteria groups.[37] Furthermore, targeted metabolomics analysis indicated that OCA could modulate host BA pool by reducing levels of serum cholic acid and chenodeoxycholic acid, and increasing levels of conjugated BAs, such as taurodeoxycholic acid and tauroursodesoxycholic acid.[37] This study demonstrated that OCA treatment changed the gut microbiota composition modulating host BAs, effectively reducing NAFLD in mice.[37] Also INT-787 modulates BA homeostasis and gut microbiota composition, leading to enhanced Verrucomicrobia and particularly *Akkermansia muciniphila*, known for improving gut homeostasis and immune functions, further indicating the crucial role of FXR activation in the protection of the small intestine against epithelial breakdown and dysbiosis.[41]

Finally, as in chronic liver diseases, NASH included, fibrosis deposition is driven by interactions among biliary epithelium and cells of the reactive stroma, mainly myofibroblasts,[25] we evaluated the expansion of the biliary cell compartment and the activation of the HPC niche. In our mouse model of NASH, treatment with both OCA and INT-787 significantly reduced the extent of pCK^+ biliary structures, similar to what observed in fibrosis Sirius red area, indicating the amelioration of liver histology. These data confirm the close relationship among ductular reaction, α-SMA levels and fibrosis development, and the positive effects of both FXR agonists in the relief of damage induced by HFD in mice.

Although this study has clearly documented the superiority of INT-787 over OCA against NASH-associated liver injury, it is limited by the lack of a dose–response study that could even more clearly support the potential therapeutic role of INT-787 also at lower doses.

In conclusion, this is the first study showing a positive effect of INT-787, greater than OCA, on restoration of hepatic RECK levels in a NASH model. These intriguing findings highlight the crucial role of MMPs and ADAMs in ECM homeostasis and the emerging role of RECK in regulating inflammatory and fibrogenic processes. Targeting RECK thus represents a promising therapeutic strategy in NASH warranting further preclinical and clinical investigations.

In addition, the beneficial effects of INT-787 on multiple parameters of metabolic regulation, the marked inhibition of liver injury, and the clear anti-inflammatory and antifibrotic effects, coupled with the favourable safety profile of the compound, indicate its potential in the treatment of other chronic liver diseases. Based on the lack of accelerated approval by the FDA of OCA for NASH treatment[3] and on common pathogenetic traits shared by NASH and alcohol-related steatohepatitis,[42] future prospects for INT-787

development will focus on the treatment of severe alcoholic hepatitis. Along these lines, a phase 2a, randomized, double-blind, placebo-controlled, dose-escalation, proof-of-concept study to evaluate the safety, tolerability, early efficacy and PK of INT-787 in subjects with severe alcohol-associated hepatitis is ongoing (ClinicalTrials.gov NCT05639543).

AUTHOR CONTRIBUTIONS

Laura G. Di Pasqua: Methodology, Formal analysis; **Marta Cagna**: Methodology, Formal analysis; **Giuseppina Palladini**: Conceptualization, Formal analysis, Writing—review and editing; **Anna C. Croce**: Conceptualization, Methodology; **Massimiliano Cadamuro**: Conceptualization, Methodology; **Luca Fabris**: Visualization; **Stefano Perlini**: Visualization; **Luciano Adorini**: Visualization; **Andrea Ferrigno**: Conceptualization, Formal analysis, Writing—original draft; **Mariapia Vairetti**: Conceptualization, Project administration, Supervision, Writing—review and editing.

FUNDING INFORMATION

This work has been supported by FRG20SZ08—University of Pavia and by Intercept Pharmaceuticals, Inc.

CONFLICT OF INTEREST STATEMENT

The authors declare no conflict of interest. The authors declare that Luciano Adorini is a part-time consultant of Intercept Pharmaceuticals. The specific role of this author is head of external preclinical research. However, except for Dr. Adorini, Intercept Pharmaceuticals did not provide support in the form of salaries for authors and did not have any additional role in the collection, analysis or interpretation of data.

DATA AVAILABILITY STATEMENT

The data presented in this study are available on request from the corresponding author.

ETHICS STATEMENT

All procedures involving animals were approved by the Italian Ministry of Health and by the University Commission for Animal Care (Protocol number 753/2020-PR).

ORCID

Giuseppina Palladini https://orcid.org/0000-0003-1312-7513
Luca Fabris https://orcid.org/0000-0001-8538-6317
Andrea Ferrigno https://orcid.org/0000-0003-2337-2897
Mariapia Vairetti https://orcid.org/0000-0002-2464-6127

REFERENCES

1. Friedman SL, Neuschwander-Tetri BA, Rinella M, Sanyal AJ. Mechanisms of NAFLD development and therapeutic strategies. *Nat Med*. 2018;24:908-922.
2. Noureddin M, Sanyal AJ. Pathogenesis of NASH: the impact of multiple pathways. *Curr Hepatol Reports*. 2018;17:350-360.
3. Adorini L, Trauner M. FXR agonists in NASH treatment. *J Hepatol*. 2023;79:1317-1331.
4. Panzitt K, Zollner G, Marschall HU, Wagner M. Recent advances on FXR-targeting therapeutics. *Mol Cell Endocrinol*. 2022;552:111678.
5. Modica S, Petruzzelli M, Bellafante E, et al. Selective activation of nuclear bile acid receptor FXR in the intestine protects mice against cholestasis. *Gastroenterology*. 2012;142:355-365.
6. Ferrigno A, Palladini G, Di Pasqua LG, et al. Obeticholic acid reduces biliary and hepatic matrix metalloproteinases activity in rat hepatic ischemia/reperfusion injury. *PLoS One*. 2020;15:1-16.
7. Duarte S, Baber J, Fujii T, Coito AJ. Matrix metalloproteinases in liver injury, repair and fibrosis. *Matrix Biol*. 2015;44–46:147-156.
8. Fiorucci S, Rizzo G, Antonelli E, et al. A farnesoid x receptor-small heterodimer partner regulatory cascade modulates tissue metalloproteinase inhibitor-1 and matrix metalloprotease expression in hepatic stellate cells and promotes resolution of liver fibrosis. *J Pharmacol Exp Ther*. 2005;314:584-595.
9. Namwat N, Puetkasichonpasutha J, Loilome W, et al. Downregulation of reversion-inducing-cysteine-rich protein with Kazal motifs (RECK) is associated with enhanced expression of matrix metalloproteinases and cholangiocarcinoma metastases. *J Gastroenterol*. 2011;46:664-675.
10. Almishri W, Swain LA, D'Mello C, Le TS, Urbanski SJ, Nguyen HH. ADAM metalloproteinase domain 17 regulates cholestasis-associated liver injury and sickness behavior development in mice. *Front Immunol*. 2022;12:779119.
11. Schmidt-Arras D, Rose-John S. Regulation of fibrotic processes in the liver by ADAM proteases. *Cell*. 2019;8:1226.
12. Müller M, Wetzel S, Köhn-Gaone J, et al. A disintegrin and metalloprotease 10 (ADAM10) is a central regulator of murine liver tissue homeostasis. *Oncotarget*. 2016;7:17431-17441.
13. Bourd-Boittin K, Basset L, Bonnier D, L'Helgoualc'h A, Samson M, Théret N. CX3CL1/fractalkine shedding by human hepatic stellate cells: contribution to chronic inflammation in the liver. *J Cell Mol Med*. 2009;13:1526-1535.
14. Dashek RJ, Diaz C, Chandrasekar B, Rector RS. The role of RECK in hepatobiliary neoplasia reveals its therapeutic potential in NASH. *Front Endocrinol (Lausanne)*. 2021;12:770740.
15. Chomczynski P, Mackey K. Substitution of chloroform by bromo-chloropropane in the single-step method of RNA isolation. *Anal Biochem*. 1995;225:163-164.
16. Roskams TA, Theise ND, Balabaud C, et al. Nomenclature of the finer branches of the biliary tree: canals, ductules, and ductular reactions in human livers. *Hepatology*. 2004;39:1739-1745.
17. Croce AC, Ferrigno A, Piccolini VM, et al. Integrated autofluorescence characterization of a modified-diet liver model with accumulation of lipids and oxidative stress. *Biomed Res Int*. 2014;2014:1-13.
18. Croce AC, Palladini G, Ferrigno A, Vairetti M. Autofluorescence label-free imaging of the liver reticular structure. *Methods Mol Biol*. 2023;2566:29-35.
19. Pellicciari R, Passeri D, De Franco F, et al. Discovery of 3α,7α,11β-trihydroxy-6α-ethyl-5β-cholan-24-oic acid (TC-100), a novel bile acid as potent and highly selective FXR agonist for enterohepatic disorders. *J Med Chem*. 2016;59:9201-9214.
20. Roth JD, Feigh M, Veidal SS, et al. INT-767 improves histopathological features in a diet-induced ob/ob mouse model of biopsy-confirmed non-alcoholic steatohepatitis. *World J Gastroenterol*. 2018;24:195-210.
21. Ganbold M, Owada Y, Ozawa Y, et al. Isorhamnetin alleviates steatosis and fibrosis in mice with nonalcoholic steatohepatitis. *Sci Rep*. 2019;9:16210.
22. Nie QH, Zhang YF, Xie YM, et al. Correlation between TIMP-1 expression and liver fibrosis in two rat liver fibrosis models. *World J Gastroenterol*. 2006;12:3044-3049.
23. Dinarello CA. Overview of the IL-1 family in innate inflammation and acquired immunity. *Immunol Rev*. 2018;281:8-27.
24. Cunningham RP, Sheldon RD, Rector RS. The emerging role of hepatocellular eNOS in non-alcoholic fatty liver disease development. *Front Physiol*. 2020;11:1-9.

25. Cadamuro M, Lasagni A, Sarcognato S, et al. The neglected role of bile duct epithelial cells in NASH. *Semin Liver Dis*. 2022;42:34-47.
26. Sinal CJ, Tohkin M, Miyata M, Ward JM, Lambert G, Gonzalez FJ. Targeted disruption of the nuclear receptor FXR/BAR impairs bile acid and lipid homeostasis. *Cell*. 2000;102:731-744.
27. Fiorucci S, Biagioli M, Baldoni M, et al. The identification of farnesoid X receptor modulators as treatment options for nonalcoholic fatty liver disease. *Expert Opin Drug Discov*. 2021;16:1193-1208.
28. Okazaki I, Noro T, Tsutsui N, et al. Fibrogenesis and carcinogenesis in nonalcoholic steatohepatitis (NASH): involvement of matrix metalloproteinases (MMPs) and tissue inhibitors of metalloproteinase (TIMPs). *Cancers (Basel)*. 2014;6:1220-1255.
29. Takahashi C, Sheng Z, Horan TP, et al. Regulation of matrix metalloproteinase-9 and inhibition of tumor invasion by the membrane-anchored glycoprotein RECK. *Proc Natl Acad Sci U S A*. 1998;95:13221-13226.
30. Oh J, Takahashi R, Kondo S, et al. The membrane-anchored MMP inhibitor RECK is a key regulator of extracellular matrix integrity and angiogenesis. *Cell*. 2001;107:789-800.
31. Peng X, Wu W, Zhu B, et al. Activation of farnesoid X receptor induces RECK expression in mouse liver. *Biochem Biophys Res Commun*. 2014;443:211-216.
32. Takagi S, Simizu S, Osada H. RECK negatively regulates matrix metalloproteinase-9 transcription. *Cancer Res*. 2009;69:1502-1508.
33. Geervliet E, Bansal R. Matrix metalloproteinases as potential biomarkers and therapeutic targets in liver diseases. *Cell*. 2020;9:1-20.
34. Radbill BD, Gupta R, Ramirez MCM, et al. Loss of matrix metalloproteinase-2 amplifies murine toxin-induced liver fibrosis by upregulating collagen I expression. *Dig Dis Sci*. 2011;56:406-416.
35. Scheller J, Chalaris A, Garbers C, Rose-John S. ADAM17: a molecular switch to control inflammation and tissue regeneration. *Trends Immunol*. 2011;32:380-387.
36. Cunningham RP, Moore MP, Dashek RJ, et al. Critical role for hepatocyte-specific eNOS in NAFLD and NASH. *Diabetes*. 2021;70:2476-2491.
37. Liu J, Sun J, Yu J, et al. Gut microbiome determines therapeutic effects of OCA on NAFLD by modulating bile acid metabolism. *NPJ Biofilms Microbiomes*. 2023;9:29.
38. Boursier J, Diehl AM. Nonalcoholic fatty liver disease and the gut microbiome. *Clin Liver Dis*. 2016;20:263-275.
39. Brandl K, Schnabl B. Intestinal microbiota and nonalcoholic steatohepatitis. *Curr Opin Gastroenterol*. 2017;33:128-133.
40. Jiao N, Loomba R, Yang ZH, et al. Alterations in bile acid metabolizing gut microbiota and specific bile acid genes as a precision medicine to subclassify NAFLD. *Physiol Genomics*. 2021;53:336-348.
41. Marzano M, Fosso B, Colliva C, et al. Farnesoid X receptor activation by the novel agonist TC-100 (3α, 7α, 11β-trihydroxy-6α-ethyl-5β-cholan-24-oic acid) preserves the intestinal barrier integrity and promotes intestinal microbial reshaping in a mouse model of obstructed bile acid flow. *Biomed Pharmacother*. 2022;153:113380.
42. Ntandja Wandji LC, Gnemmi V, Mathurin P, Louvet A. Combined alcoholic and non-alcoholic steatohepatitis. *JHEP Reports Innov Hepatol*. 2020;2:2.

SUPPORTING INFORMATION

Additional supporting information can be found online in the Supporting Information section at the end of this article.

How to cite this article: Di Pasqua LG, Cagna M, Palladini G, et al. FXR agonists INT-787 and OCA increase RECK and inhibit liver steatosis and inflammation in diet-induced ob/ob mouse model of NASH. *Liver Int*. 2024;44:214-227. doi:10.1111/liv.15767